System-Wide Harmonic Mitigation in a Diesel Electric Ship by Model Predictive Control

Espen Skjong, Jon Are Suul, *Member, IEEE*, Atle Rygg, Tor Arne Johansen, *Senior Member, IEEE*, and Marta Molinas, *Member, IEEE*

***Abstract*—This paper proposes a system-oriented approach for mitigating harmonic distortions by utilizing a single Active Power Filter (APF) in an electrical grid with multiple buses. Common practice for control of APFs is to locally compensate the load current harmonics or to mitigate voltage harmonics at a single bus. However, the operation of an APF in a multi-bus system will influence the voltages at neighboring buses. It is therefore possible to optimize the APF operation from a system perspective instead of considering only conventional local filtering strategies. For such purposes, Model Predictive Control (MPC) is proposed in this paper as a framework for generating APF current references that will minimize the harmonic distortions of the overall system within a given APF rating. A diesel-electric ship, with two buses supplying separate harmonic loads, with an APF located at one of the buses, is used as study case. The operation with on-line MPC-based optimization of the APF current references is compared to two benchmark methods based on conventional approaches for APF control. The results demonstrate that the MPC generates current references that better utilize the APF current capability for system-wide harmonic mitigation.**

***Index Terms*—Active Power Filter (APF), Optimization, Model Predictive Control (MPC), System-Wide Harmonic Mitigation, Total Harmonic Distortion (THD)**

Manuscript received September 3, 2015; revised December 22, 2015; accepted January 15, 2016.

This work has been carried out at the Centre for Autonomous Marine Operations and Systems (AMOS). The Norwegian Research Council is acknowledged as the main sponsor of AMOS. This work was supported by Ulstein Power & Control AS and the Research Council of Norway, Project number 241205.

E. Skjong is with the Department of Engineering Cybernetics, Norwegian University of Science and Technology, 7034 Trondheim, Norway, with the Centre for Autonomous Marine Operations and Systems (AMOS), Norwegian University of Science and Technology, 7052 Trondheim, Norway, and also with Ulstein Power & Control AS, 6018 Ålesund, Norway (e-mail: espen.skjong@ulstein.com)

J. A. Suul is with the Department of Electric Power Engineering, Norwegian University of Science and Technology, 7495 Trondheim, Norway, and also with SINTEF Energy Research, 7465 Trondheim, Norway (e-mail: jon.are.suul@ntnu.no)

A. Rygg is with the Department of Engineering Cybernetics, Norwegian University of Science and Technology, 7034 Trondheim, Norway, (e-mail: atle.rygg@itk.ntnu.no)

T. A. Johansen is is with the Department of Engineering Cybernetics, Norwegian University of Science and Technology, 7034 Trondheim, Norway, and also with the Centre for Autonomous Marine Operations and Systems (AMOS), Norwegian University of Science and Technology, 7052 Trondheim, Norway, (e-mail: tor.arne.johansen@itk.ntnu.no)

M. Molinas is with the Department of Engineering Cybernetics, Norwegian University of Science and Technology, 7034 Trondheim, (e-mail: marta.molinas@ntnu.no)

I. Introduction

HARMONICS are any deviation from the pure sinusoidal voltage or current waveform typically generated by an ideal voltage source with linear loads [1]. In a diesel-electric ship power system, the main source of harmonics is usually the diode rectifier stages of Variable Frequency Drives (VFDs) for controlling the propulsion motors. A wide variety of VFDs are in use today depending on the power level, the pulse-number of the rectifiers and the system design, each of them generating different harmonic distortion levels [2]–[4].

Harmonic distortions in a power system can be mitigated by installing passive filter solutions (i.e. inductive and capacitive filters) that will reduce the impact of harmonic load currents on the rest of the system. For large nonlinear loads with known harmonic spectra, tuned harmonic filters for dominant low-order components are commonly applied [5], [6]. Such configurations can also include high-pass filters for mitigating a wider range of higher order harmonics. However, passive filters must be carefully designed to avoid resonances causing amplification of other harmonic components, especially when the installation is exposed to parameter variations or frequent changes in system configuration [7]. Furthermore, the amplitude of the harmonic current components generated by a diode rectifier will depend on the active power needed by the loads. Thus, a set of shunt-connected passive filters cannot be effectively adapted to the wide range of variations in propulsion loads on-board an electrical ship. Another alternative for passive harmonic mitigation is to apply series connected wide spectrum filters [3]. However, such filters must be installed in each of the propulsion loads, and will not mitigate harmonics generated by smaller VFD loads in the system.

High harmonic distortion levels in a system with dominant VFD loads can also be avoided by applying Active Rectifiers (ARs) instead of diode rectifiers. However, this solution is still more costly and has also higher losses than passive rectifiers. Another option to deal with harmonics without resorting to passive filters or diode rectifiers with high pulse numbers and complex multi-winding transformers for all VFD loads, is the use of Active Power Filters (APFs). The common practice in active filtering is to use the APF for local compensation by applying a current reference equal to the harmonic and reactive current components of the non-linear load [1]. However, when there are multiple non-linear loads distributed on multiple buses in a system, like in a marine vessel grid, minimizing the total harmonic distortion in the system will no longer be possible with the local filtering approach. In such grid configurations, with several and dispersed sources of harmonics,

approaches for controlling APFs with the objective of system-wide harmonic mitigation represents an interesting option that has not yet been systematically pursued.

Optimization techniques can provide a general framework for generating optimal current reference waveforms for an APF with the objective of minimizing the overall total harmonic distortion (THD) in a system. Significant research efforts have recently been directed towards application of Model Predictive Control (MPC) to the local control of power electronic converters, including APFs [8], [9]. However, the potential for utilizing MPC in system-wide harmonic mitigation with an APF still remains to be exploited.

In this paper, application of MPC is thoroughly investigated for system-wide harmonic conditioning with a shunt-connected Voltage Source Converter (VSC), controlled as an APF, based on the original idea presented in [10]–[12]. The previously presented studies on this topic were preliminary explorations of the capability of the MPC for minimizing the total harmonic voltage distortion (THD_V) in the load buses of a marine vessel power grid, based on simplified models with ideal current sources. Although the results in [10]–[12] indicated that APF current references generated by a system-wide MPC-based approach can improve the THD_V at the main buses compared to local filtering approaches, the impact of accurate load models and the implementation of the APF were not taken into account. A revised and improved closed-loop implementation of MPC for optimal harmonic mitigation is presented in this paper, and demonstrated in a model of a marine vessel power grid implemented in MATLAB/Simulink with detailed models of VFD rectifiers and the APF. The APF performance with the proposed system-wide control approach is compared to the results with traditional local filtering and an ad-hoc solution proposed in [13]. The same trend as observed in the previous works is confirmed, with consistently improved system-level THD_V when the MPC approach is used to calculate the APF current references. Furthermore, the results highlight the advantages of the MPC compared to the solution from [13], namely the higher degree of freedom and flexibility, the ability to impose APF current saturation (constraints) and the ability to find an optimal current reference for an APF in a complex power grid with more than two buses.

II. Marine Vessel's Power Grid

Diesel-electric power generation and propulsion for marine vessels was commercialized and fully adopted by the offshore industry in the mid 1990s, with industry partners for power solutions at the helm. For an offshore operation vessel, the power demand, i.e. the vessel's power profile, is given by the vessel's momentarily assignment, e.g. transit, station keeping with Dynamic Positioning (DP) or anchor-handling. Diesel-electric vessels have introduced a flexibility of power generation when needed, compared to mechanical drive vessels where the prime mover is directly connected to the propeller via mechanical gears and long shafts. Therefore, diesel-electric operation has contributed to cultivating a *green environment* philosophy where the fuel consumption, and thus the exhaust emission, is in line with the power demand [2]. Diesel-electric power generation has also introduced advanced redundant power grid designs, e.g. ring bus designs, which satisfy requirements set by classification entities, such as ABS, Lloyd's Register and DNV GL [14]. This favors an increased number of installed generators with lower power ratings, facilitating a more *step-less* power generation compared to vessels with redundant mechanical drives.

The power grid under investigation in this work is based on a simplified equivalent of a marine Platform Supply Vessel (PSV) power system with two buses and two propulsion loads, operating with closed bus-tie breaker. The simplification is justified from the fact that these loads are typically responsible for the dominant part of the power consumption and the dominant harmonic distortions. A single-line diagram of the assumed power grid configuration is shown in Fig. 1. In the investigated operating conditions, the vessel has only two generators in operation, one connected to each bus, *Bus 1* and *Bus 2*, respectively, since this is assumed to be the worst case for voltage distortions in the system. One propulsion motor supplied through a VFD is connected to each bus. The VFD has either a 6-pulse or a 12-pulse diode rectifier interfaced to the bus, and a voltage source inverter for controlling the motor driving the propeller. A transformer is included to provide galvanic isolation and for phase shifting in case of a 12-pulse rectifier. A series impedance is included between the two buses. Finally, the active filter is connected to bus 2 as seen in the Fig. 1. Table I lists the most important details of the power grid under investigation, where the adopted pu base values are referred to the generator ratings.

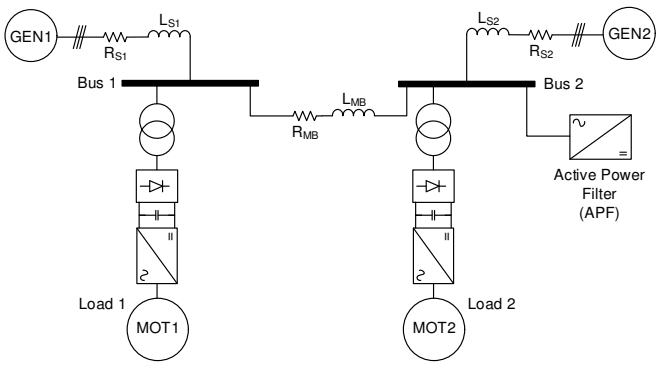

Fig. 1. Simplified diagram of the power grid under investigation, including two generators, two loads and an active power filter.

TABLE I
Power grid parameters, with generator rating as pu-base.

Parameter	Value		
L_{S1}	20% [pu]	**Generator 1**	1MVA
L_{S2}	20% [pu]	**Generator 2**	1MVA
L_{MB}	4% [pu]	**Motor 1**	1MVA
R_{S1}	$10\% \cdot L_{S1} \cdot \omega$ [pu]	**Motor 2**	1MVA
R_{S2}	$10\% \cdot L_{S2} \cdot \omega$ [pu]	**Active filter**	200kVA
R_{MB}	$10\% \cdot L_{MB} \cdot \omega$ [pu]	**Voltage (RMS)**	690V, 50Hz

The maximum allowed total harmonic distortion in a marine vessel's power system is regulated by classification entities. DNV GL follows IEC 61000-2-4 Class 2, which implies that the total harmonic voltage distortion (THD_V) shall not

exceed 8% [15]. In addition, DNV GL requires that no single order harmonic voltage component shall exceed 5%. Similarly, Lloyd's Register requires that the THD_V at any ac switchboard or section board is below 8% (unless specified otherwise) of the fundamental, considering all frequencies up to 50 times the supply frequency. Within this requirement, no voltage component at a frequency above 25 times the supply frequency should exceed 1.5% of the fundamental of the supply voltage [16]. American Bureau of Shipping (ABS) recommends that the THD_V should not exceed 5%, as measured at any point of common coupling (PCC), with any individual harmonic voltage not exceeding 3% of the fundamental voltage value. The range of harmonics to be taken into account should be up to the 50th harmonic [17]. Bureau Veritas (BV) has similar rules and regulations [18]. However, the classification entities do not provide a clear set of requirements regarding total harmonic current distortion (THD_I) at any specific points, as harmonic current distortions do not propagate the power grid as easily as harmonic voltage distortions due to impedances in the system. Thus, this work will focus on harmonic voltage distortions at the main buses of the system, intending to comply with the classification requirements according to ABS.

III. Model Predictive Control

In this paper, Model Predictive Control (MPC) is utilized to achieve optimal APF control for system-wide selective harmonic mitigation in a power grid, by generating APF current references optimized within the APFs current rating [10]–[12]. The main idea of MPC is to calculate the control action for a process/system using a (usually simplified) model to predict the system's future behavior. The model is initialized by measurements of the system's current state, and at each sampling interval the control action is obtained by solving online a constrained finite horizon optimal control problem [19]. The control action is extracted from the resulting finite control sequence yielded from the optimization and given to the system to close the control loop. Depending on the MPC's computational costs, there might be a non-negligible time delay between the initialization of the model and the resulting calculated control sequence, which must also be taken into account in the implementation.

The MPC's accuracy and computational costs are dependent on the model of the system and the availability and accuracy of real-time measurements. To model a system perfectly is in most cases an impossible task. In addition, modelling all dynamics, if possible, usually result in a large and complex model with high computational costs, that often requires more measurements. Therefore, a compromise between accuracy and computational costs must be made when designing MPC schemes. In general, the model applied for MPC should be as simple as possible while containing all dynamics needed to satisfy the control objective within the control horizon and the level of discretization. The horizon's length is dependent on the control objective, and the level of discretization should be chosen with respect to the fastest dynamics that should be controlled. A thorough overview of dependable embedded MPCs is given in [20].

In the literature it has been reported MPC implementations with good real-time properties [21]–[23], and some research has also been conducted to explore the use of optimization and MPC in the field of electrical engineering [9], [24], [25]. The MPC formulation described in this section is based on the models and approaches from [10], [11] and [12]. However, the implementation and the formulation of the objective function are further improved to benefit from the MPC's flexibility in the search for the optimal filter current injection. In the following, the power grid model and the active filter constraints used in the development of the MPC are discussed before the MPC formulation is presented on standardized form.

A. Power Grid Model

As mentioned, MPC depends on a model of the system for calculating the optimal control actions. The main 690V busbars and loads in diesel-electric ships are usually three-phase three-wire systems. Thus, there will be no path for zero-sequence currents and the system could be modelled in the $\alpha\beta$ frame (by using the Clarke transform) while ignoring zero sequence components [1]. This would imply a reduced dimension of the problem formulation for the MPC compared to modelling in the abc frame, and could be beneficial for reducing computational costs (for real-time implementation). However, representation in the $\alpha\beta$ frame implies that the current limit of the APF in the α-axis will depend on the current in the β-axis and vice versa. Since functionality for such limitations are not included in the MPC software used in this work, the MPC formulation will be based on the abc frame. In the following, subscript a, b and c are used to denote the abc phases of each voltage and current component. The vectors $\mathbf{v}$ and $\mathbf{i}$ are used to represent the voltages and currents, respectively, given in the abc frame.

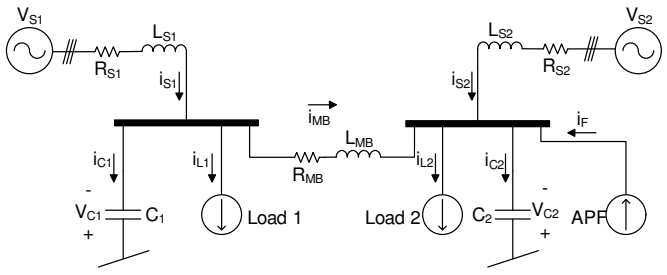

Fig. 2. Simplified power grid model used to design the MPC for harmonic mitigation.

Fig. 2 shows a simplified power grid model approximating the marine vessel's power grid discussed in section II, with parameters adopted from Table I. The shunt capacitors indicated in the figure are included to decouple the states representing currents in the inductances, but can also be considered as an equivalent representation of the cable and busbar capacitances. The capacitor voltage states will represent the busbar voltages used for assessing the THD_V in the system.

In this work, a simplified generator model with fixed voltage amplitude behind an impedance is used for the modelling and simulations. The per unit generator impedance is selected to

be within the normal range for sub-transient reactances of synchronous machines, according to [26]. A constant fundamental frequency model is also assumed, i.e. $\omega := 2\pi f(t) = 2\pi f$ where f is the nominal fundamental frequency. In reality, the frequency of a ship power system will not be constant and the synchronous generators will have voltage controller dynamics as well as small internal voltage distortions due to the physical construction. However, the applied simplified model can be considered sufficient to demonstrate the steady state system-wide optimization achieved with the MPC without depending on simulations with large mechanical and electromechanical time constants. The MPC is also partly able to reject unmodelled disturbances since the internal system model will be continuously updated through closed-loop feedback. Furthermore, the MPC can easily handle frequency variations as long as the harmonic analysis in the control system is frequency-adaptive. If necessary, a simple dynamic frequency model, can also be embedded in the MPC, as proposed in [10].

Assuming 6-pulse rectifiers are part of the marine vessel's propulsion system, the loads will introduce non-linear conditions drawing harmonic current of order 5, 7, 11, 13, etc. from the generators [1]. Hence, the load model used in the MPC can be modeled as ideal current sources,

$$\mathbf{i}_L(t) = \begin{bmatrix} i_{L,a}(t) \\ i_{L,b}(t) \\ i_{L,c}(t) \end{bmatrix} = \begin{bmatrix} \sum_i I_{L,i} \sin\left(i\left(\omega t + \phi_{L,i}\right)\right) \\ \sum_i I_{L,i} \sin\left(i\left(\omega t + \phi_{L,i} - \frac{2\pi}{3}\right)\right) \\ \sum_i I_{L,i} \sin\left(i\left(\omega t + \phi_{L,i} + \frac{2\pi}{3}\right)\right) \end{bmatrix}, \quad \forall i \in \{6k \pm 1 | k = 1, 2, \ldots\}, \tag{1}$$

which includes the assumed harmonic components, i, to be mitigated, with phase shifts $\phi_{L,i}$ and amplitudes $I_{L,i}$. Note that the load model, (1), does not include the fundamental current components. If the marine vessel's power grid includes elements that generate other dominant harmonic components, the load models and the harmonics to be mitigated by the MPC can be changed accordingly.

The APF in Fig. 2 should be controlled to suppress the harmonic content of the generator currents in order to minimize the voltage harmonics at the main buses. The APF currents in all three phases, $i_{F,a}$, $i_{F,b}$ and $i_{F,c}$, are kept as free variables and are optimally calculated by the MPC. This decision gives total authority to the MPC, allowing the MPC to phase shift and alter the different harmonic components of the filter currents in any possible way to achieve the best possible harmonic mitigation. This is an important property when the APF is reaching its peak current limits.

The power grid's dynamics can be derived using Kirchhoff's laws and be stated as

$$L_{S1}\frac{d\mathbf{i}_{S1}}{dt} = -R_{S1}\mathbf{i}_{S1} - \mathbf{v}_{C1} \tag{2a}$$

$$C_1\frac{d\mathbf{v}_{C1}}{dt} = \mathbf{i}_{S1} - \mathbf{i}_{MB} - \mathbf{i}_{L1} \tag{2b}$$

$$L_{MB}\frac{d\mathbf{i}_{MB}}{dt} = \mathbf{v}_{C1} - \mathbf{v}_{C2} - R_{MB}\mathbf{i}_{MB} \tag{2c}$$

$$C_2\frac{d\mathbf{v}_{C2}}{dt} = \mathbf{i}_{MB} + \mathbf{i}_{S2} - \mathbf{i}_{L2} + \mathbf{i}_F \tag{2d}$$

$$L_{S2}\frac{d\mathbf{i}_{S2}}{dt} = -R_{S2}\mathbf{i}_{S2} - \mathbf{v}_{C2}. \tag{2e}$$

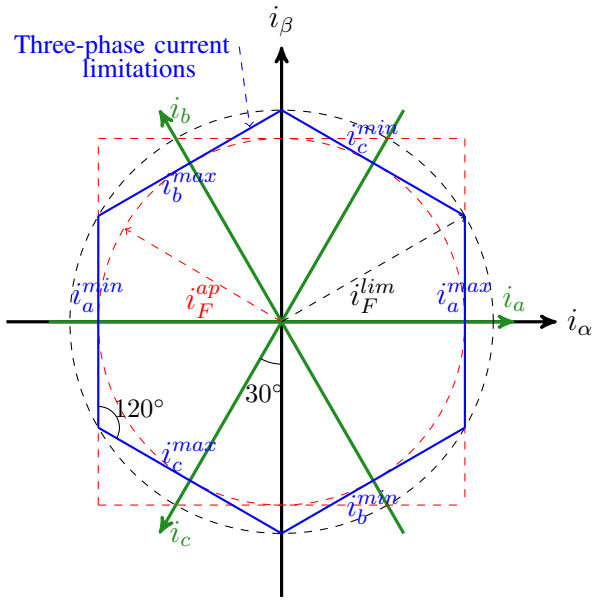

Fig. 3. Active power filter constraints: Three-phase three-wire system represented in the $\alpha\beta$ and abc frames [27].

As seen from these equations, the bus voltages are provided in the model by the capacitances, and the differences between the two bus voltages determine the current flowing in the main bus impedance ($\mathbf{i}_{MB}$). For the MPC implementation, (2) does not include the fundamental components since the MPC only regards harmonic components. It should also be mentioned that potential voltage distortions originating from the generators or from other components in the systems that are difficult to measure, will affect the harmonic generator currents. Thus, the MPC will indirectly attenuate the effect of such disturbances since they will be contained by the feedback signals used to initialize the internal model of the MPC.

B. Active Power Filter Constraints

The APF's current and voltage limits are determined by its physical components. In general, the semiconductor devices, usually IGBT modules containing anti-parallel diodes, determine the current rating, while the voltage rating of the dc-side capacitor limits the maximum voltage available to inject current harmonics into the grid. The current limitations will be the same for all three phases, as illustrated in the abc frame by the blue hexagon in Fig. 3 [27]. These limits should be included in the MPC formulation to avoid unwanted effects from saturation of filter current references (i.e. current clipping). Inclusion of the current limits in the MPC will also ensure that the utilization of the current capability will be optimized. By this, the MPC will be able to optimally calculate APF currents close to the APF's limits without saturation effects impairing the harmonic conditioning.

The current constraints given by the hexagon in Fig. 3 can be formulated in the abc frame as

$$i^{min} \leq i_j \leq i^{max}, \quad \forall j \in \{a, b, c\}, \tag{3}$$

where $i^{min} = -i^{max}$. The constraints given in $\alpha\beta$ form can be found in [10]–[12].

As mentioned, the MPC model could be developed in the $\alpha\beta$ frame for a more effective implementation of the system model. However, the implementation of the current constrains are more complicated in the $\alpha\beta$ frame. Therefore, it is preferred in this case to implement the MPC in the abc frame. For notational simplicity the set of feasible filter currents given by the constraints defined in (3) is in the following denoted $\mathbb{S}$.

C. Formulating the MPC on Standard Form

With the formulation of the model and the APF's constraints, which was discussed in section III-A and III-B, the MPC at time t with a control horizon of length T can be written on standard form as

$$\begin{aligned}\min_{\mathbf{x}(t),\mathbf{z}(t),\mathbf{u}(t)} \quad & V(\mathbf{x}(t),\mathbf{z}(t),\mathbf{u}(t)) = \\ & \int_{t_0}^{t_0+T} l\left(\mathbf{x}(t),\mathbf{z}(t),\mathbf{u}(t)\right) dt \\ \text{s.t.} \quad & \\ & \dot{\mathbf{x}}(t) = \mathbf{f}\left(\mathbf{x}(t),\mathbf{z}(t),\mathbf{u}(t)\right), \\ & \mathbf{g}\left(\mathbf{x}(t),\mathbf{z}(t),\mathbf{u}(t)\right) = 0, \\ & \mathbf{h}\left(\mathbf{x}(t),\mathbf{z}(t),\mathbf{u}(t)\right) \leq 0, \\ & \forall t \in [t_0, t_0+T] \wedge \mathbf{x}(t_0), \mathbf{z}(t_0) | \mathbf{i}_F(t_0) \in \mathbb{S},\end{aligned} \tag{4}$$

where $V(\cdot)$ is the objective function defining the objective of the optimization, $l(\cdot)$ is the stage cost function and $\mathbf{f}(\cdot)$ represents the power grid's dynamics given by (2). $\mathbf{g}(\cdot)$ represents the MPC's equality constraints, in which includes algebraic equations such as the load models given by (1). $\mathbf{h}(\cdot)$ represents the MPC's inequality constraints, which includes the filter's current limits given by (3). The dynamic state vector, $\mathbf{x}$, is given by the power grid's dynamic equations, and by omitting the time notation (t), it can be stated as

$$\mathbf{x} = \left[\mathbf{i}_{S1}^\top, \mathbf{i}_{S2}^\top, \mathbf{i}_{MB}^\top, \mathbf{v}_{C1}^\top, \mathbf{v}_{C2}^\top\right]^\top, \tag{5}$$

where $\mathbf{i}_{S1}$ and $\mathbf{i}_{S2}$ are the harmonic generator (source) currents to be compensated, $\mathbf{i}_{MB}$ is the main bus current and $\mathbf{v}_{C1}$ and $\mathbf{v}_{C2}$ are the bus voltages in Fig. 2. The load currents $\mathbf{i}_{L1}$ and $\mathbf{i}_{L2}$ can be expressed by the algebraic state vector $\mathbf{z}$,

$$\mathbf{z} = \left[\mathbf{i}_{L1}^\top, \mathbf{i}_{L2}^\top\right]^\top. \tag{6}$$

The control vector, $\mathbf{u}$, which consists of the filter currents, is given by

$$\mathbf{u} = \mathbf{i}_F = \left[i_{F,a}, i_{F,b}, i_{F,c}\right]^\top. \tag{7}$$

The objective of the MPC is to conduct selective harmonic mitigation in the power grid. Harmonic pollution may induce vibrations and torque changes in the generator shafts, depending on the generators' inductance. To reduce wear and tear on the generators, the harmonics in the generator currents (source currents $\mathbf{i}_{S1}$ and $\mathbf{i}_{S2}$) should be compensated. A convex stage cost function which addresses the harmonic pollution in the generator currents can be stated as

$$\begin{aligned} l\left(\mathbf{x},\mathbf{z},\mathbf{u}\right) = & \mathbf{i}_{S1}^\top \mathbf{Q}_1 \mathbf{i}_{S1} \\ & + \mathbf{i}_{S2}^\top \mathbf{Q}_2 \mathbf{i}_{S2} \\ & + \left(\mathbf{i}_{F,a} + \mathbf{i}_{F,b} + \mathbf{i}_{F,c}\right)^\top \mathbf{Q}_{abc} \left(\mathbf{i}_{F,a} + \mathbf{i}_{F,b} + \mathbf{i}_{F,c}\right) \\ & + \mathbf{u}^\top \mathbf{Q}_u \mathbf{u}, \end{aligned} \tag{8}$$

with diagonal weight matrices given by

$$\begin{aligned} &\mathbf{Q}_1 = \text{diag}([q_1, q_1, q_1]),\ \mathbf{Q}_2 = \text{diag}([q_2, q_2, q_2]), \\ &\mathbf{Q}_u = \text{diag}([q_u, q_u, q_u]),\ \mathbf{Q}_{abc} = \text{diag}([q_{abc}, q_{abc}, q_{abc}]). \end{aligned} \tag{9}$$

The last part in (8) is added to punish utilization of large filter currents (amplitudes), which will make it easier for the MPC to use phase shifting in the search of the optimal harmonic mitigation [11]. The third part is added to avoid solutions that relies on zero-sequence filter currents. Because punishment of large filter currents is of lesser importance than minimization of the harmonic pollution and avoiding optimal solutions that rely on zero-sequence filter currents, the weights should be selected so that $q_{abc} > q_1, q_2 > q_u$. Since the load model in (1) as used by the MPC does not include the fundamental components, the objective is to minimize the source current, where perfect harmonic cancellation would yield $\mathbf{i}_{S1} = \mathbf{i}_{S2} = \mathbf{0}^{3\times 1}$.

The weighting of the harmonics from the different buses, q_1 and q_2, could be modified to also include a weighting relative the amount of harmonics originating from each load, i.e.

$$\begin{aligned} q_1 &= k_1 \cdot \sum_i I_{L1,i} \\ q_2 &= k_2 \cdot \sum_i I_{L2,i}, \end{aligned} \tag{10}$$

where k_1 and k_2 are weighting constants and i are the harmonics to be mitigated. In this way, the MPC could be designed for prioritizing harmonic mitigation on the most polluted bus, or according to any other criteria suitable for a specific system. However, further discussions or analysis of such possibilities are outside the scope of this work.

IV. Implementation

With references to section II and section III, where the power grid and the MPC formulation were presented, respectively, the implementation of the simulation environment will be discussed in this section. Before discussing the closed-loop interaction between the MPC and the power grid, the power grid simulation model and the MPC implementation are separately addressed.

A. Power Grid Implementation

The power grid, which was presented in Fig. 1 with properties given in Table I, is implemented in MATLAB/Simulink using the SimPowerSystems library. For ensuring fast and robust current reference tracking in a simple way, the APF control is based on a traditional phase current hysteresis controller [28], [29]. The hysteresis band is in this case set

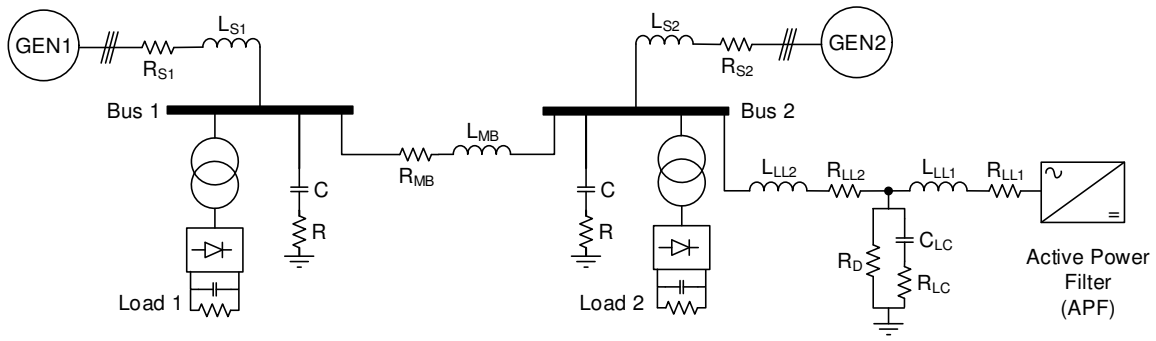

Fig. 4. Power grid implementation in MATLAB/Simulink, with parameters given in Table I and Table II.

to 0.15 [pu] (relative the APF's rating), and the resulting average switching frequency is approximately 17.5kHz. The active filter's DC link voltage reference is set to approximately 1240V ($1.1 \cdot 2 \cdot \frac{\sqrt{2}}{\sqrt{3}} \cdot 690V$), and a PI controller is used to control the DC link toward its reference [1]. An LCL filter with passive damping is inserted between the active filter and bus 2 to suppress switching noise from the active filter. To avoid unrealistic high frequency oscillations in the system, the parasitic bus capacitances are modelled as shunt RC elements placed on each side of the bus-tie connection. An illustration of the power grid implementation is given in Fig. 4, with the most important parameters listed in Table I and Table II.

TABLE II
POWER GRID IMPLEMENTATION DETAILS.

Parameter	Value
AF DC link	1240V
AF DC capacitor	236μF
AF hysteresis frequency	$\approx$ 17.5kHz
AF hysteresis band	0.15 [pu] (relative APF rating)
Shunt RC	$R = 2\Omega$, $C = 1\mu$F
LCL filter	$L_{LL1} = L_{LL2} = 0.4$mH, $R_{LL1} = R_{LL2} = 0.02\Omega$, $C_{LC} = 40\mu$F, $R_D = 120\Omega$, $R_{LC} = 10\Omega$

B. MPC Implementation

The MPC formulation addressed in this work is implemented using the software environment ACADO (Automatic Control and Dynamic Optimization) [30], which is a higher-level toolkit than the CasADi framework [31] used in [10]–[12]. Using ACADO, the MPC formulations are implemented in standard form, and the toolkit builds the MPC using user-specified shooting techniques, e.g. single shooting, multiple shooting or collocation [32], and solvers such as qpOASES [33]. The ACADO toolkit also provides a code-generation tool for generating efficient MPC-implementations in C and MATLAB [34]. The main reason why ACADO is used in this work to realize the MPC is the toolkit's fast prototyping properties and the code-generation feature, which can generate an efficient MATLAB implementation of the MPC and make the integration with the power-grid implementation in MATLAB/Simulink less cumbersome. The main details of the MPC implementation are listed in Table III.

As indicated in Table III, the MPC's optimization horizon is set to 12.5ms, which is slightly longer than half a period for the fundamental frequency of 50Hz. Even though the fundamental period is 20ms, the MPC is set to run every 10th ms to achieve a faster closed-loop feedback and be able to correct for model/process mismatches. Thus, only the first 10ms of the MPC's resulting control horizon will be used to provide an optimal APF current reference. The additional 2.5ms are included to keep future changes in account, and provide an overlap between the control horizons. This is an important property for achieving continuous optimality between each MPC cycle [19].

TABLE III
MPC IMPLEMENTATION DETAILS.

Parameter	Value
Time horizon T	12.5ms
Discretization N	220
Discretization type	Multiple Shooting
Integrator	Runge-Kutta 4 (RK4)
Hessian Approximation ($\nabla^2_{\mathbf{x}}\mathbf{f}(\cdot)$)	Exact Hessian
Solver	qpOASES
Number of iterations	5
Stage cost weights	$q_1 = q_2 = 1000$, $q_u = 1$, $q_{abc} = 0$
AF current limit	$i_F^{ap} = 1[pu]$ (of APF rating)

The filter currents in the MPC model are kept as free variables, as was described in section III-A, giving the MPC full flexibility and authority when searching for the optimal harmonic mitigation. Hence, the quality of the harmonic mitigation is dependent on the MPC's discretization. In addition, the level of discretization has significant influence on the MPC's real-time properties. However, details regarding real-time implementation of the MPC on suitable industrial control platforms is outside the scope of this study. In the following, the discretization is chosen to be 220 samples for each 12.5ms, which gives a discretization step-size that allows for reasonably accurate analysis up to about the 37th harmonics.

C. Closing the Control Loop

Using the MPC and the power grid model, a closed loop APF control for system-wide harmonic mitigation can be obtained. A block diagram illustrating the simulated system is given in Fig. 5. Instantaneous measurements are used to initialize the MPC's internal model before each new cycle. The **FFT** (moving horizon) block is used to extract measurements, i.e. amplitudes and phase angles, from the load currents,

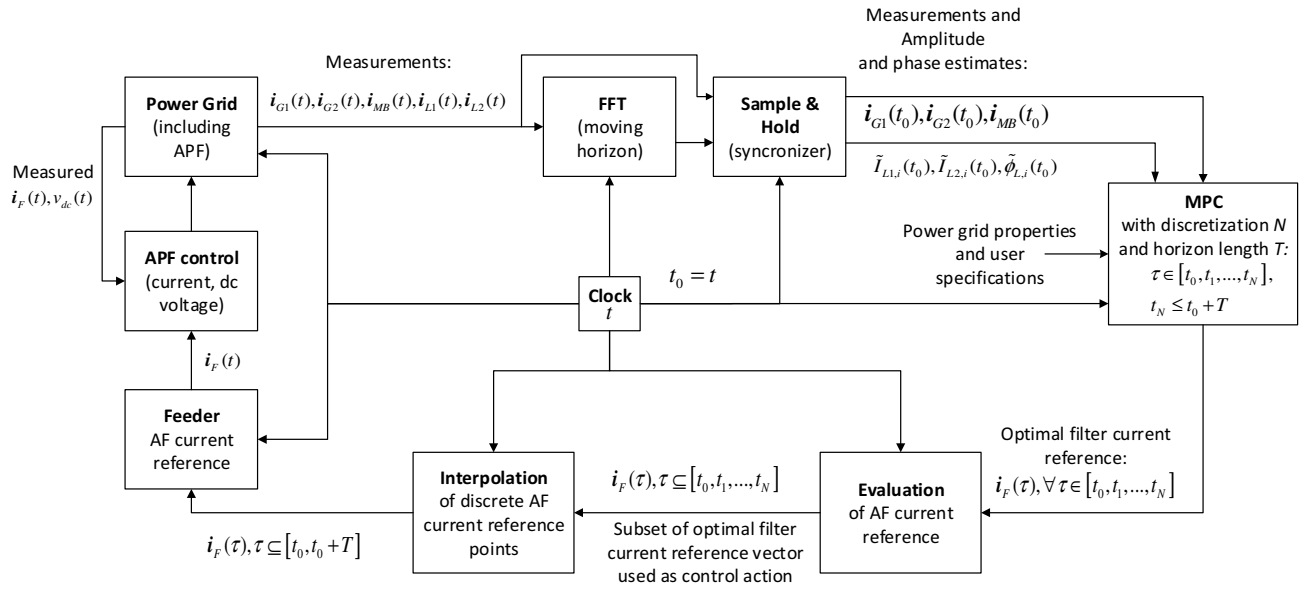

Fig. 5. Functional overview of the closed-loop implementation in MATLAB/Simulink.

originating from the **Power Grid** block. The output from the **FFT** block and the instantaneous measurements are sampled with the same clock signal as the rest of the system in the **Sample & Hold** block, which synchronizes the measurements with the MPC. The output from the **MPC** block is discrete filter currents (vectors) in the abc frame. These vectors are sent to the **Evaluation** block which ensures that the filter currents are within the APF's constraints. As filter current references containing zero-sequence components cannot be tracked by the APF, any zero-sequence components are removed from the current references before they are provided to the APF's hysteresis controllers. As an alternative to use the zero-sequence penalty in the MPC's objective function, which was given as the third term of (8), the **Evaluation** block is equipped with additional functionality that transforms the filter current references to the $\alpha\beta 0$ frame, where the zero-sequence current components are removed. The APF's constraints, which were shown in Fig. 3, are imposed before transforming the resulting filter current references back to abc form. Since zero-sequence current components are equal for all three-phase [1], the elimination of zero-sequence currents will not destroy the optimality of the filter current reference calculated by the MPC.

TABLE IV
CLOSED LOOP IMPLEMENTATION DETAILS.

Parameter	Value
MPC cycle	100Hz
Power grid simulation step-size	2μs

After evaluating the filter currents, the **Evaluation** block extracts a subset of the filter currents to be used. The length of the extracted subset is relative the MPC's run cycle. The subset of the filter current vector is then sent to the **Interpolation** block, which interpolates the points in the filter current vectors to get the same discretization as used in the simulation environment. The resulting filter current vectors are sent to the **Feeder** block, which feeds the **APF control** block with one point (one for each phase) at the time. The **APF control** block includes the local control loops used to operate the APF in the power grid, including phase current hysteresis controllers and a dc-voltage PI controller providing the fundamental frequency active current reference. A global clock is used in the simulation to synchronize all time dependent blocks, including the electrical system. The MPC's run cycle and the simulation step-size are given in Table IV.

V. RESULTS

To validate the selective harmonic conditioning using the MPC formulation discussed in section III, two methods for active filter current reference generation are applied as benchmark cases:

- BM1: $\mathbf{i}_F = \mathbf{i}_{L2}^h$
- BM2: $\mathbf{i}_F = \mathbf{i}_{L1}^h + \mathbf{i}_{L2}^h$,

where $\mathbf{i}_{L1}^h$ and $\mathbf{i}_{L2}^h$ are the selected harmonic currents from load 1 and load 2 in the abc frame, respectively, to be suppressed by the active filter. As can be seen, BM1, which is named *local filtering* in [10]–[12], only considers the load connected to the same bus as the APF. This approach is considered as a standard strategy for harmonic mitigation. The second benchmark case, BM2, is an ad-hoc method for harmonic mitigation in a two-bus system proposed in [13]. This approach attempts to mitigate the harmonics in the system by using the sum of the harmonic content from both loads as the current reference for the APF. Thus, the grid impedances are not considered, and this approach will only obtain a direct compensation of the load harmonics if the bus impedance is zero. It should be noted that this approach is not established or commonly applied for APF control in multi-bus systems but it is included as a reference case for providing a more fair

basis of comparison for the MPC than what is achieved with BM1.

Three different study cases are simulated for the two benchmark models and the proposed MPC:

1) **Bus 1:** 6-pulse rectifier load. **Bus 2:** 6-pulse rectifier load. The loads have equal power demand.
2) **Bus 1:** 12-pulse rectifier load. **Bus 2:** 6-pulse rectifier load. The load at bus 1 has higher power demand than the load at bus 2.
3) **Bus 1:** 12-pulse rectifier load in parallel to a single-phase rectifier load. **Bus 2:** 6-pulse rectifier load. The aggregated loads at bus 1 has higher power demand than the load at bus 2.

The configuration of the power grid used in the simulations was given in Table I, and the harmonic components to be mitigated are the 5th, 7th, 11th and 13th. The 5th and 7th harmonic components will be the dominant harmonics in a load with a 6-pulse rectifier while the 11th and 13th harmonic components are dominant in a load consisting of a 12-pulse rectifier. The filter current limits for harmonic current injection are set to 1 [pu] in all phases (referred to the APF rating), as mentioned in Table III. For each case the resulting THD_V values averaged for all three phases of each bus and key information about the system configuration are summarized in tables, and two figures are presented: The first two plots in the first figure showing the filter output current (measured after the LCL filter) and its reference, while the two last plots show the resulting generator currents. All results are plotted only for phase a. The second figure shows the frequency spectra of the bus voltages and generator currents for phase a up to the 50th harmonic - all harmonics given in percentage of the fundamental component. The results from each case are discussed in the following.

A. Study Case 1

The first study case is a scenario where both loads are equal, both with 6-pulse rectifiers, and connected to the grid. As shown in Table V, the power demands from each load are set to 5% of their power ratings. As expected, the THD_Vs presented in Table V for BM1 and BM2 are not equal as BM1 only considers harmonic mitigation for bus 2 while BM2 considers both buses. As BM1 only considers the local load connected to bus 2, harmonic currents from load 1 will be unsuppressed and flow through the grid, from one bus to the other, resulting in higher THD_Vs than BM2 and the MPC. BM2 is in this case better than BM1 due to its consideration of the selected harmonics to be suppressed from both loads. However, due to the lack of information of the power grid's configuration, BM2 is not able to match the THD_Vs resulting from the optimal harmonic mitigation using the MPC. The reason why can be seen from the two upper plots in Fig. 6a, where the APF current with MPC is slightly phase shifted and has a slightly lower amplitude compared to the APF current with BM2. This is mainly because the MPC is explicitly considering the impedances in the system. The resulting APF current from BM1 has lower harmonic amplitudes compared to the MPC and BM2, since it is only compensating for the harmonic currents generated by load 1.

TABLE V
STUDY CASE 1: CONFIGURATION AND RESULTING THD_V.

	MPC	BM1	BM2
THD $\mathbf{V}_{L1}$	1.4%	2.9%	1.6%
THD $\mathbf{V}_{L2}$	1.4%	2.6%	1.8%
Load 1 element	6-pulse		
Load 2 element	6-pulse		
Power load 1	0.05 [pu]		
Power load 2	0.05 [pu]		

The two lower plots in Fig. 6a show the generator currents with harmonic conditioning according to all three methods. As shown, the generator currents are quite similar for BM2 and the MPC, while they are significantly more distorted with BM1. This is as expected, since the BM1 is not compensating for the harmonic load currents at bus 1.

The two upper plots in Fig. 6b show the frequency spectra of the bus voltages while the two lower plots show the frequency spectra of the generator currents up to the 50th harmonic component. For the bus 1 voltage, the MPC is better than BM1 for almost all the harmonics. Compared to BM2, the MPC gives a slightly higher magnitude for the 5th, 7th and 13th harmonic, however, results in lower magnitudes for all other dominating harmonic components. This is due to the fact that the MPC penalizes filter currents which introduce harmonics that is not part of the harmonic suppression in the grid. This can be seen from (8), where all filter currents corresponding to non-zero generator harmonics are penalized. For the bus 2 voltage the MPC seems to result in lower magnitudes than BM1 and BM2 for all dominating harmonic components. As evident, BM1 has the highest magnitudes in both voltage spectra, indicating higher THD_V than both the MPC and BM2. As the load demands from both loads are quite small, the THD_I is quite high for the generator currents, which can be observed from the two lower plots in Fig. 6b.

B. Study Case 2

The second study case is a scenario where load 1 has a 12-pulse diode rectifier and load 2 has a 6-pulse rectifier. The power demand from load 1 is set higher than the power demand from load 2, as indicated in Table VI, with power demands of 80% and 30% of rated load, respectively. The THD_Vs presented in Table VI show that also in this case the BM2 is providing superior performance compared to BM1, since the harmonic components in load 1 have significant impact on the bus voltages. However, the MPC is able to improve the harmonic mitigation beyond what is achievable with BM2, further decreasing the THD_Vs at both buses. It can be noticed that in this case BM1 violates the ABS classification requirement of THD_V below 5%, and the individual harmonic limits are also exceeded for the 11th and the 13th harmonic voltage components at bus 1, see Fig. 7b.

As in the previous case, the filter current resulting from BM1 deviates from BM2 and the MPC due to the local filtering approach, which can be seen from Fig. 7a. The difference between the filter currents from BM2 and the MPC is also in

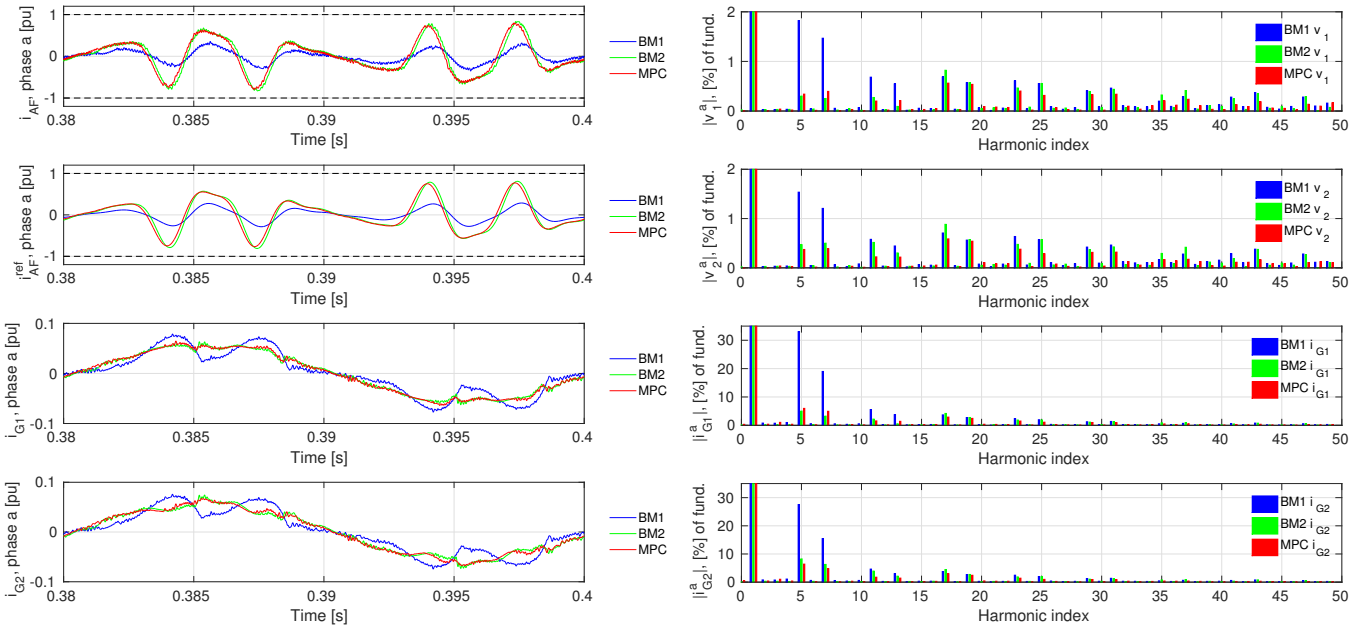

(a) Filter and generator currents. (b) Load voltage and generator current frequency spectra.

Fig. 6. Study case 1: Two loads with 6-pulse rectifiers and equal power demand, one load connected to each bus.

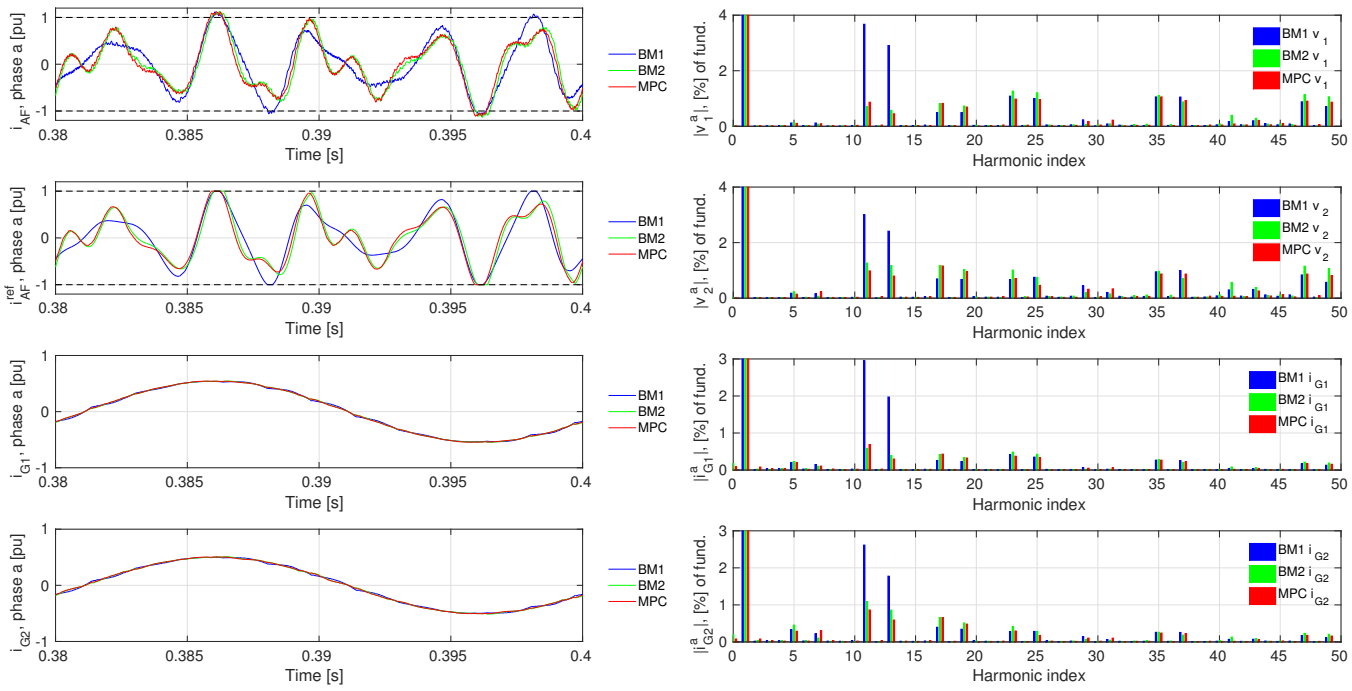

(a) Filter and generator currents. (b) Load voltage and generator current frequency spectra.

Fig. 7. Study case 2: One load with a 12-pulse rectifier connected to bus 1 and one load with a 6-pulse rectifier connected to bus 2. The power demand from load 1 is higher than the power demand from load 2.

this case given by a small phase shift and a small difference in amplitude. From the two upper plots in Fig. 7b it is seen that the MPC has lower magnitudes for all dominating harmonic components in the bus 1 voltage compared to BM2, except the 11th and 37th harmonic components. Hence, the MPC compromises and scarifies the 11th harmonic component in the bus 1 voltage to decrease the THD_V in bus 2 beyond the abilities of BM2. This is seen in the spectra for the bus 2 voltage, where the magnitude of almost all dominating harmonic components are lower for the MPC compared to BM2. The spectra for the generator currents in the lower two plots in Fig. 7b show some of the same behavior, resulting in lower THD_Is for both generator currents when using the MPC for harmonic mitigation compared to BM1 and BM2.

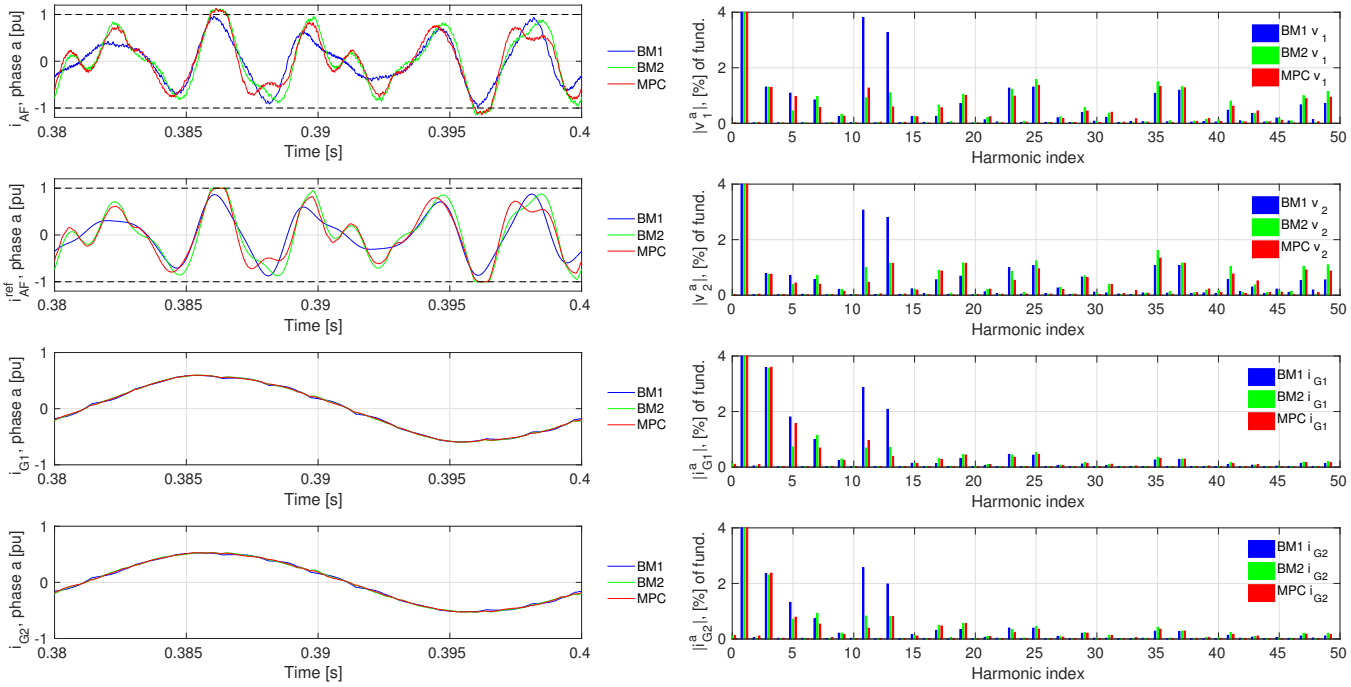

(a) Filter and generator currents.

(b) Load voltage and generator current frequency spectra.

Fig. 8. Study case 3: A three-phase load with a 12-pulse rectifier and a single-phase load with a 2-pulse rectifier connected to bus 1. One three-phase load with a 6-pulse rectifier connected to bus 2. The aggregated power demand from load 1 is higher than the power demand from load 2.

TABLE VI
STUDY CASE 2: CONFIGURATION AND RESULTING THD_V.

	MPC	BM1	BM2
THD $\mathbf{V}_{L1}$	2.8%	5.3%	3.1%
THD $\mathbf{V}_{L2}$	2.8%	4.5%	3.4%
Load 1 element	12-pulse		
Load 2 element	6-pulse		
Power load 1	0.8 [pu]		
Power load 2	0.3 [pu]		

TABLE VII
STUDY CASE 3: CONFIGURATION AND RESULTING THD_V.

	MPC	BM1	BM2
THD $\mathbf{V}_{L1}$	3.9%	6.0%	4.2%
THD $\mathbf{V}_{L2}$	3.5%	5.0%	4.0%
Load 1 element	12-pulse + single-phase 2-pulse		
Load 2 element	6-pulse		
Power load 1	0.8 [pu] + 0.1 [pu]		
Power load 2	0.25 [pu]		

C. Study Case 3

The third study case illustrates the performance of the three different harmonic mitigation approaches with an additional aggregation of single-phase loads on bus 1, resulting in unbalanced conditions. The power demands from bus 1 are 80% for the three-phase 12-pulse load and in total 10% for aggregated single-phase diode rectifier loads (phase a and b). This results in a load current unbalance of about 6% on bus 1. The power demand from the three-phase 6-pulse load in bus 2 is 25%. The resulting THD_Vs for the three different harmonic mitigation methods are given in Table VII, and also in this case there are clear distinctions between the methods. As in the previous study cases the MPC conducts the best harmonic mitigation while BM1 conducts the worst. Evidently, BM1 violates also in this case the classification requirement of THD_V below 5%.

Compared to the previous study cases, the difference between the APF reference currents generated by the three methods are now easier to recognize, as illustrated in the two upper plots in Fig. 8a. Differences between the three APF reference currents in both phase angles and amplitudes are easily recognized from the plot, indicating different results from the harmonic mitigation, which is supported by the resulting THD_Vs in Table VII.

The frequency spectra in Fig. 8b show the presence of zero-sequence harmonics, e.g. 3rd and 9th, which is a result of the unbalanced conditions caused by the single-phase diode rectifier load connected to bus 1. From the spectra of bus voltage 1, the MPC results in lower magnitudes compared to BM2 for all dominating harmonic components, except for the 5th and 11th component. Also from the spectra of bus voltage 2, the MPC has lower dominating harmonic magnitudes than BM2, except for the 5th harmonic component. From both voltage spectra it is easy to see that BM1 results in the worst harmonic mitigation, where the 11th and 13th components are major contributors to the increased THD_V compared to the MPC and BM2. Also in this case the 3% single harmonic voltage limit set by some of the classification entities is violated by BM1.

The results in this section indicate that the use of MPC can provide better system-level harmonic mitigation than both BM1 and BM2. The results also demonstrate that BM2, which is used in this work as a reference for comparison, is not

an optimal solution, especially when there is non-negligible impedances between the buses in the system and when the APF current saturation is reached. Furthermore, the results demonstrate that the MPC can achieve better utilization of an APF within its current limitations.

VI. Conclusion

An approach for system-wide harmonic mitigation using Model Predictive Control (MPC) to generate the current reference for an active power filter (APF) has been presented and implemented in this paper. Three case-studies of non-linear load conditions in a ship power system with two separate buses have been implemented in a MATLAB/Simulink model, and the compensation performance obtained with the MPC-based control is compared to two control techniques based on conventional filtering strategies. The THD_Vs obtained with system-oriented on-line optimization with the MPC are the lowest among the three cases investigated. The presented results highlight the advantages of the MPC over conventional approaches; namely its higher degree of freedom when dynamically searching the optimal values by treating all selected harmonics at once without restricting the APF current references by a direct mathematical relation to the load currents, and the ability to optimize within APF current limits (constraints). In particular, the MPC has advantages when the available current from the APF is constrained by the current rating of the converter. Although the results presented in this paper are obtained in a system with only two separate buses, the MPC algorithm can easily be extended to account for a larger system configuration. Thus, the use of the MPC or another formal optimization technique for online system-wide harmonic mitigation can be clearly beneficial compared to conventional approaches for generating APF current references. This will especially be the case when the complexity of the electrical grid increases, and when the APF operation is constrained by its current ratings. The approach presented in this manuscript can also be applied to other APF topologies, or it can be included in active rectifiers or inverters with multi-functional control capabilities.

References

[1] H. Akagi, E. Watanabe, and M. Aredes, *Instantaneous Power Theory and Applications to Power Conditioning*. Wiley, 2007.

[2] M. Patel, *Shipboard Electrical Power Systems*. Taylor & Francis, 2011.

[3] I. Evans, A. Hoevenaars, and P. Eng, "Meeting harmonic limits on marine vessels," in *IEEE Electric Ship Technologies Symposium, 2007. ESTS '07*, May 2007, pp. 115–121.

[4] S. Gleaves and G. Perla, "Electric propulsion, it's time to get onboard," Maritime Reporter and Engineering News, 2009.

[5] R. P. Stratford, "Harmonic Pollution on Power Systems - A Change in Philosophy," *IEEE Trans. Ind. Appl.*, vol. IA-16, no. 5, pp. 617–623, September/October 1980.

[6] S. M. Peeran and C. W. P. Cascadden, "Application, Design, and Specification of Harmonic Filters for Variable Frequency Drives," *IEEE Trans. Ind. Appl.*, vol. 31, no. 4, pp. 841–847, July/August 1995.

[7] C.-J. Wu, J.-C. Chiang, S.-S. Yen, C.-J. Liao, J.-S. Yang, and T.-Y. Guo, "Investigation and Mitigation of Harmonic Amplification Problems Caused by Single-tuned Filters," *IEEE Trans. Power Del.*, vol. 13, no. 3, pp. 800–806, July 1998.

[8] P. Cortés, M. P. Kazmierkowski, R. M. Kennel, D. E. Quevedo, and J. Rodríguez, "Predictive control in power electronics and drives," *IEEE Trans. Ind. Electron.*, vol. 55, no. 12, pp. 4312–4324, December 2008.

[9] T. Geyer, G. Papafotiou, and M. Morari, "Model predictive control in power electronics: A hybrid systems approach," in *44th IEEE Conference on Decision and Control 2005, and 2005 European Control Conference. CDC-ECC '05.*, Dec 2005, pp. 5606–5611.

[10] E. Skjong, M. Molinas, and T. A. Johansen, "Optimized current reference generation for system-level harmonic mitigation in a diesel-electric ship using non-linear model predictive control," in *IEEE ICIT 2015 International Conference on Industrial Technology*, March 2015.

[11] E. Skjong, M. Molinas, T. A. Johansen, and R. Volden, "Shaping the current waveform of an active filter for optimized system level harmonic conditioning," in *VEHITS 2015 International Conference on Vehicle Technology and Intelligent Transport Systems*, May 2015.

[12] E. Skjong, M. Ochoa-Gimenez, M. Molinas, and T. A. Johansen, "Management of harmonic propagation in a marine vessel by use of optimization," in *2015 IEEE Transportation Electrification Conference and Expo 2015 (ITEC 2015)*, March 2015.

[13] A. Rygg Aardal, E. Skjong, and M. Molinas, "Handling system harmonic propagation in a diesel-electric ship with an active filter," in *ESARS 2015 Conference on Electrical Systems for Aircraft, Railway, Ship Propulsion and Road Vehicles*, March 2015.

[14] "DNVGL-OS-D201: Offshore standards, Electrical Installations," July 2015.

[15] "DNV-RU-SHIP-Pt4Ch8: Part 4 Systems and components, Chapter 8 Electrical installations," October 2015.

[16] "Lloyd's Register: General Information for the Rules and Regulations for the Classification of Ships," July 2014.

[17] "ABS: Guidance Notes on Control of Harmonics in Electrical Power Systems," May 2006.

[18] "Bureau Veritas: Rules for the Classification of Steel Ships: Part C - Machinery, Electricity, Automation and Fire Protection," July 2014.

[19] J. Rawlings and D. Mayne, *Model Predictive Control: Theory and Design*. Nob Hill Pub., 2009.

[20] T. Johansen, "Toward dependable embedded model predictive control," *IEEE Syst. J.*, vol. in press, no. 99, pp. 1–12, 2014.

[21] K. Ling, S. Yue, and J. Maciejowski, "A FPGA implementation of model predictive control," in *American Control Conference, 2006*, June 2006, pp. 6 pp.–.

[22] F. Xu, H. Chen, W. Jin, and Y. Xu, "FPGA implementation of nonlinear model predictive control," in *The 26th Chinese Control and Decision Conference (2014 CCDC),*, May 2014, pp. 108–113.

[23] G. Frison, D. Kwame Minde Kufoalor, L. Imsland, and J. Jørgensen, "Efficient implementation of solvers for linear model predictive control on embedded devices," in *Proceedings of 2014 IEEE International Conference on Control Applications (CCA)*, 2014, pp. 1954–1959.

[24] P. Lezana, R. Aguilera, and D. Quevedo, "Model predictive control of an asymmetric flying capacitor converter," *IEEE Trans. Ind. Electron.*, vol. 56, no. 6, pp. 1839–1846, June 2009.

[25] A. Garces, M. Molinas, and P. Rodriguez, "A generalized compensation theory for active filters based on mathematical optimization in ABC frame," *Electric Power Systems Research, Elsevier Journal*, vol. 90, no. 0, pp. 1 – 10, 2012.

[26] N.-Q. Dinh and J. Arrilaga, "A Salient-Pole Generator Model for Harmonic Analysis," *IEEE Trans. Power Syst.*, vol. 16, no. 4, pp. 609–615, November 2001.

[27] J. A. Suul, "Control of Grid Integrated Voltage Source Converters under Unbalanced Conditions," PhD thesis, Norwegian University of Science and Technology, Department of Electrical Power Engineering, March 2012.

[28] D. M. Brod and A. W. Novotny, "Current Control of VSI-PWM Inverters," *IEEE Trans. Ind. Appl.*, vol. IA-21, no. 4, pp. 562–570, May/June 1985.

[29] M. P. Kaźmierkowski and L. Malesani, "Current Control Techniques for Three-Phase Voltage Source PWM Converters: A Survey," *IEEE Trans. Ind. Electron.*, vol. 45, no. 5, pp. 691–703, October 1998.

[30] B. Houska, H. Ferreau, and M. Diehl, "ACADO Toolkit – An Open Source Framework for Automatic Control and Dynamic Optimization," *Optimal Control Applications and Methods*, vol. 32, no. 3, pp. 298–312, 2011.

[31] J. Andersson, "A General-Purpose Software Framework for Dynamic Optimization," PhD thesis, Arenberg Doctoral School, KU Leuven, Department of Electrical Engineering (ESAT/SCD) and Optimization in Engineering Center, Kasteelpark Arenberg 10, 3001-Heverlee, Belgium, October 2013.

[32] L. Biegler, *Nonlinear Programming: Concepts, Algorithms, and Applications to Chemical Processes*. Society for Industrial and Applied Mathematics (SIAM, 3600 Market Street, Floor 6, Philadelphia, PA 19104), 2010.

[33] H. Ferreau, C. Kirches, A. Potschka, H. Bock, and M. Diehl, "qpOASES: A parametric active-set algorithm for quadratic programming," *Mathematical Programming Computation*, vol. 6, no. 4, pp. 327–363, 2014.
[34] B. Houska, H. Ferreau, and M. Diehl, "An Auto-Generated Real-Time Iteration Algorithm for Nonlinear MPC in the Microsecond Range," *Automatica*, vol. 47, no. 10, pp. 2279–2285, 2011.

Espen Skjong received his MSc degree in Engineering Cybernetics at the Norwegian University of Science and Technology (NTNU), Trondheim, Norway, in 2014, specializing in model predictive control (MPC) for autonomous control of UAVs. He is currently employed in Ulstein Power & Control AS (Ålesund, Norway) as an industrial PhD candidate. His research topic is optimization in power management systems for marine vessels. His industrial PhD fellowship is within the Center of Excellence on Autonomous Marine Operations and Systems (AMOS) at NTNU.

Jon Are Wold Suul (M'11) received the MSc and PhD degrees from the Department of Electric Power Engineering at the Norwegian University of Science and Technology (NTNU), Trondheim, Norway, in 2006 and 2012, respectively. From 2006 to 2007, he was with SINTEF Energy Research, Trondheim, where he was working with simulation of power electronic converters and marine propulsion systems, until starting his PhD studies. In 2008, he was a guest PhD student for two months with the Energy Technology Research Institute of the National Institute of Advanced Industrial Science and Technology (AIST), Tsukuba, Japan. He was also a visiting PhD student for two months with the Research Center on Renewable Electrical Energy Systems, within the Department of Electrical Engineering, Technical University of Catalonia (UPC), Terrassa, Spain, during 2010. Since 2012, he has resumed a part-time position as a Research Scientist at SINTEF Energy Research while also working as a part-time postdoctoral researcher at the Department of Electric Power Engineering of NTNU. His research interests are mainly related to control of power electronic converters in power systems and for renewable energy applications.

Atle Rygg received his MSc from the Department of Electrical Power Engineering at the Norwegian University of Science and Technology (NTNU), Trondheim, Norway, in 2011. From August 2011 to December 2014, he was with SINTEF Energy Research, Trondheim, Norway. He is currently employed as a PhD-candidate with the Department of Engineering Cybernetics at NTNU. His main field of research is real-time monitoring of stability in power electronic dominated systems. This includes detection of harmonic resonances as well as interactions between different subsystems.

Tor Arne Johansen (M'98, SM'01) received the MSc degree in 1989 and the PhD degree in 1994, both in electrical and computer engineering, from the Norwegian University of Science and Technology (NTNU), Trondheim, Norway. From 1995 to 1997, he worked at SINTEF as a researcher before he was appointed Associated Professor at NTNU in Trondheim in 1997 and Professor in 2001. He has published several hundred articles in the areas of control, estimation and optimization with applications in the marine, automotive, biomedical and process industries. In 2002 Johansen co-founded the company Marine Cybernetics AS where he was Vice President until 2008. Prof. Johansen received the 2006 Arch T. Colwell Merit Award of the SAE, and is currently a principal researcher within the Center of Excellence on Autonomous Marine Operations and Systems (AMOS) and director of the Unmanned Aerial Vehicle Laboratory at NTNU.

Marta Molinas (M'94) received the Diploma degree in electromechanical engineering from the National University of Asuncion, Asuncion, Paraguay, in 1992; the Master of Engineering degree from Ryukyu University, Japan, in 1997; and the Doctor of Engineering degree from the Tokyo Institute of Technology, Tokyo, Japan, in 2000. She was a Guest Researcher with the University of Padova, Padova, Italy, during 1998. From 2004 to 2007, she was a Postdoctoral Researcher with the Norwegian University of Science and Technology (NTNU) and from 2008-2014 she has been professor at the Department of Electric Power Engineering at the same university. From 2008 to 2009, she was a Japan Society for the Promotion of Science (JSPS) Research Fellow with the Energy Technology Research Institute, National Institute of Advanced Industrial Science and Technology, Tsukuba, Japan. In 2014, she was Visiting Professor at Columbia University and Invited Fellow by the Kingdom of Bhutan working with renewable energy microgrids for developing regions. She is currently Professor at the Department of Engineering Cybernetics, NTNU. Her research interests include stability of power electronics systems, harmonics, oscillatory phenomena, and non-stationary signals from the human and the machine. Dr. Molinas has been an AdCom Member of the IEEE Power Electronics Society. She is Associate Editor and Reviewer for *IEEE Transactions on Power Electronics* and *PELS Letters*.